

Theoretical and experimental study on the effect of nitrogen content on the thermal characteristics of nitrocellulose under low heating rates

Hua Chai · Qiangling Duan · Lin Jiang · Liang Gong · Haodong Chen ·
Jinhua Sun 

Received: 16 January 2018 / Accepted: 22 October 2018 / Published online: 31 October 2018
© Springer Nature B.V. 2018

Abstract The thermal behavior of nitrocellulose (NC) with different nitrogen contents has been widely investigated in previous works. However, most of the experiments were carried out under high heating rates, a situation in which it is difficult to capture minor changes during the thermal decomposition process. In the present study, the thermal characteristics of NC with different nitrogen contents were theoretically and experimentally investigated using a CALVET heat flux calorimeter C80 at heating rates from 0.2 to 0.8 °C/min. Before thermal analysis, the results of high-precision scanning electron microscopy showed that more cracks

and coarser surfaces were detected on NC fibers with higher nitrogen contents. It was found that a “turning point” was detected on the heat flow curves of NC with higher nitrogen contents. Furthermore, the heat flow curves of NC transformed from “bell shape” to “right triangles” with increases in the nitrogen content, which suggested that NC with high nitrogen contents exhibited autocatalysis characteristics under low heating rates. This characteristic was also confirmed by the isothermal experiment results that showed the autocatalytic properties became increasingly obvious by increasing the isothermal temperature. Moreover, the relevant chemical kinetic and thermodynamic parameters were obtained. The heat of the reaction (ΔH) increased and the activation energy values in the initial stages of NC decomposition decreased as the nitrogen content was increased. Furthermore, the critical explosion temperature (T_b), which is as an important parameter to evaluate the thermal hazard of NC, decreased by elevating the nitrogen content.

H. Chai · Q. Duan (✉) · L. Jiang · L. Gong ·
H. Chen · J. Sun (✉)
State Key Laboratory of Fire Science, University of
Science and Technology of China, Hefei 230026, People’s
Republic of China
e-mail: duanql@ustc.edu.cn

J. Sun
e-mail: sunjh@ustc.edu.cn

H. Chai
xc30@mail.ustc.edu.cn

Q. Duan
e-mail:

L. Jiang
e-mail: jianglin@ustc.edu.cn

L. Gong
e-mail: gl409418@mail.ustc.edu.cn

H. Chen
e-mail: linghao@ustc.edu.cn

Keywords Nitrocellulose · Nitrogen content ·
Thermal characteristic · Microstructure · Low heating
rate · Thermal explosion temperature

Introduction

As a derivative of cellulose, nitrocellulose (NC) has been widely used in industrial and military

applications, including uses as celluloid, lacquers and solid rocket propellants (Shao and Wang 2011; Zhang et al. 2014; Cuissinat et al. 2008; Zhou et al. 2016; Krause 2013; Trache et al. 2016; Weir 1946; Lin et al. 2016). However, nitrocellulose exhibits some unique hazardous properties, such as high impact sensitivity, poor chemical stability, flammability and explosive hazards. In particular, heat accumulation will occur in the NC system if the heat production rate is much higher than the heat release rate, and ultimately thermal runaway may occur (Wang et al. 2012). As a result, catastrophic fire or explosions are more likely to happen (Jiang et al. 2018).

Several major accidents caused by NC degradation are summarized in Table 1 (Xinhua News Agency 2016; Sun and Ding 2007). Among these accidents, a particularly significant fire explosive disaster occurred at Tianjin port in China, which caused 165 deaths, 8 missing people and 798 injuries. The direct cause of the accident was the loss of the wetting agent for the nitrocellulose, resulting in local desiccation and heat accumulation due to exposure to the sun in summer for long periods and the poor heat dissipation in the containers (Xinhua News Agency 2016). Therefore, in order to understand and maintain appropriate safety protocols, it is necessary to understand the thermal characteristics and thermal hazards during nitrocellulose transport and storage.

Recently, many investigations (Pourmortazavi et al. 2009; Sovizi et al. 2009; Katoh et al. 2010; He et al. 2017; Wei et al. 2017) have been performed to study the thermal characteristics, microstructures,

chemical kinetics and thermodynamics of NC. The effects of nitrogen content on the thermal decomposition of NC under high heating rates, ranging from 5 to 20 °C/min in helium atmospheres, were analyzed. It has been concluded that the thermal stability decreased with an increase in nitrogen content (Pourmortazavi et al. 2009). In another study, the thermal behaviors and microstructures of microsized and nanosized NC were compared, this proved that the nanosized NC was more dangerous. Additionally, the relevant kinetics were obtained by using ASTM E969 and the Ozawa method (Sovizi et al. 2009). In an air atmosphere, a small exothermic peak was detected before the main exothermic one on heat flow curves of NC and NC stabilized with diphenylamine (DPA) or akardite II (AKII) under a heating rate of 0.02 °C/min (Katoh et al. 2010). The effects of humectants on thermal stability, microstructure and combustion characteristics of NC were investigated (He et al. 2017), which proved that NC with isopropanol and ethanol humectants showed minor differences in their microstructures, but the former possessed a larger fire risk. Finally, exterior structures showed certain influences on the fire properties of NC, for example, the chip NC was proven to possess a lower fire hazard when compared with the soft fiber NC (Wei et al. 2017).

The majority of previous studies have focused on thermal characteristics of NC at high heating rates (ranging from 5 to 20 °C/min). In practice, NC slowly decomposes and releases heat at 40 °C (Xinhua News Agency 2016). Lower heating rates compared with

Table 1 Major accidents related to nitrocellulose (NC) during storage or handling processes (Xinhua News Agency 2016; Sun and Ding 2007)

Number	Category	Time	Site	Cause	Result
1	Nitrocellulose	1874	England	The accumulation of nitrocellulose caused spontaneous combustion	More than 20 deaths
2	Celluloid	1927	Soviet Union	Film fires caused the disaster	144 deaths
3	Celluloid	1952	Japan	Spontaneous combustion of a toy made of celluloid	14 deaths and 21 injuries
4	Celluloid	1974	Japan	Film spontaneous combustion caused the fire	More than 3000 films burned
5	Explosives	2011	Cyprus	Two boxes of gunpowder fire caused an explosion	13 deaths
6	Nitrocellulose	2016	China	The wetting agent loss of NC was the main reason for the spontaneous combustion	165 deaths, 8 missing people and 798 injuries

higher ones can capture more details and minor changes of the NC decomposition process. Moreover, it is widely known that the hazard degree is closely related to the nitrification degree (or nitrogen content). Nevertheless, many scientific issues remain unsolved in the understanding of the thermal characteristics of nitrocellulose with different nitrogen contents under low heating rates, such as microcosmic structure, peak shape, reaction characteristics and relevant kinetic parameters. Therefore, in the present study, theoretical and experimental studies were carried out to reveal the effects of nitrogen content on the thermal characteristics of nitrocellulose under low heating rates. C80 calorimeter, a kind of thermal analysis technique, has been used isothermally and non-isothermally in the study of the NC decomposition kinetics (Abd-Elghany et al. 2017). SEM are performed to compare their microstructures of NC with different nitrogen content. To obtain the kinetics parameter variations at different reaction stages for NC with different nitrogen contents, an advanced model free method has been employed. Compared with the model-fitting method that uses only single heating rate, the isoconversional methods using multiple heating rate programs not only can circumvent the methodological flaws but also give more reliable kinetic parameters, which has been recommended by the international confederation for thermal analysis and calorimetry (ICTAC) (Vyazovkin et al. 2011; Trache 2016; Trache et al. 2017). And kinetic investigation of energetic materials is crucial since it helps to understand the thermal decomposition characteristics, and to deeply evaluate the effect of exothermic decomposition on the potential hazard in handling, processing, storage and use (Trache et al. 2018). Commonly, several parameters are necessary to be evaluated. For example, the released heat per unit sample mass of NC samples were derived. The heating rates and characteristics temperatures were extracted from experimental heat flow curves, based on which the critical thermal runaway temperatures were also induced for different NC samples. In addition, to characterize their auto-catalytic processes, a series of isothermal experiments were performed on C80 calorimeter with selection of 150 and 175 °C isothermal processes.

Materials and methods

Material preparation and sample labeling

In our experiments, four kinds of NC materials were selected. Their nitrogen contents are 11.43% (NC-11.43), 11.50% (NC-11.50) 11.98% (NC-11.98) and 12.87% (NC-12.87). All NC samples were provided by the Borui chemical raw materials plant in Guangdong Province. Before the experiment, all the materials were placed in a vacuum dryer to prevent interference from other factors. Figure 1 shows the macrostructures of NC with different nitrogen contents, which present similar whiteness and powdered soft fibers such as those of cellulose.

Measuring apparatus

SEM

The differences in physical microstructures of the four samples were determined by using a scanning electron microscope (SEM). Scanning electron micrographs were recorded by means of a Philips XL30 ESEM-TMP SEM (Netherlands) with an accelerating voltage of 10 kV.

C80 micro calorimeter

A C80 micro calorimeter is commonly used as an appropriate tool to evaluate thermal characteristics of various kinds of substances (Wu et al. 2018; Wang et al. 2006; Onésippe et al. 2010; Mundhwa and Henni 2007; Bessières et al. 2005; Miyake et al. 2000; Vincent et al. 2017). Heat flow curves of nitrocellulose were derived from a CALVET heat flux calorimeter C80, manufactured by SETARAM Scientific & Industrial Equipment Company in France. The schematic of the apparatus is presented in Fig. 2; a CS32 controller was connected to the computer to record the experimental data, and a 3D sensor inside surrounded the samples to maintain stable heating conditions. The calorimeter has a high sensitivity (with a limit of 1 μ W) and a wide testing temperature range from room temperature to 300 °C. The weighed sample needed to be sealed into the sample cell. At the same time, there needed the same mass of alumina for the reference cell. The schematic of the sample cell and the reference cell is shown in Fig. 3. Additionally, the

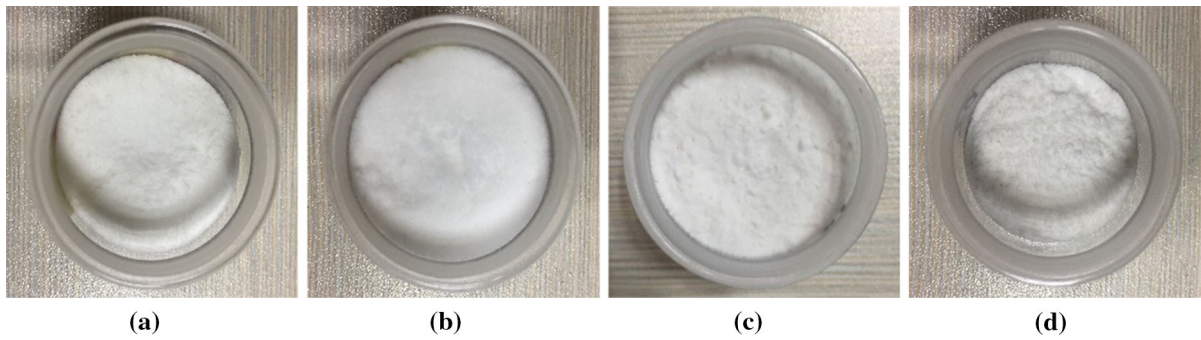


Fig. 1 Macrostructures of NC with different nitrogen content, **a** 11.43% (NC-11.43), **b** 11.50% (NC-11.50) **c** 11.98% (NC-11.98) and **d** 12.87% (NC-12.87)

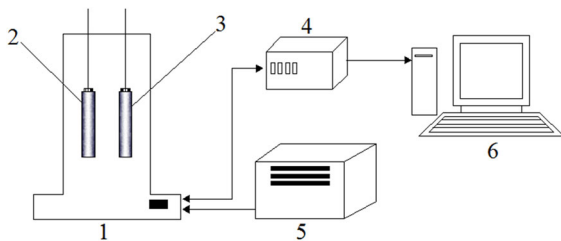


Fig. 2 Schematic of the C80 microcalorimeter: (1) high-precision reactor, (2) reaction cell, (3) reference cell, (4) CS32 control system, (5) power supply system, (6) data collection system

sample cell is made of stainless steel (Z2 CND 17–12) and made up with a cylindrical container and a cap, whose volume is 8.5 mL. The same mass of alumina for the reference cell was guaranteed for each experiment.

Experimental methods

To obtain more details on the thermal characteristics of NC with four levels of nitrogen content, non-isothermal and isothermal methods were applied in the experiments. For the nonisothermal experiments, the heating rates used in this study were approximately 25–100 times lower than those in previous works by others (Pourmortazavi et al. 2009; Sovizi et al. 2009; He et al. 2017), namely, 0.2, 0.4, 0.6, and 0.8 °C/min, from room temperature to 300 °C. For the isothermal experiments, the executed program has four segments in total. The first part is the initial stabilization phase with the stable time of 1800 s at around 30 °C; the second part is the heating stage, the temperature rises from 30 °C to a set constant temperature (150 and 175 °C) with 1 °C/min heating rate; the third part is the constant temperature stage and the maintained stable time is 40,000 s; and the last one is the cooling stage, which is cooled from the set temperature to 30 °C with the cooling rate of 0.9 °C/min. Data in the third stage were chosen to identify if the reaction possessed autocatalytic characteristics. Finally, the

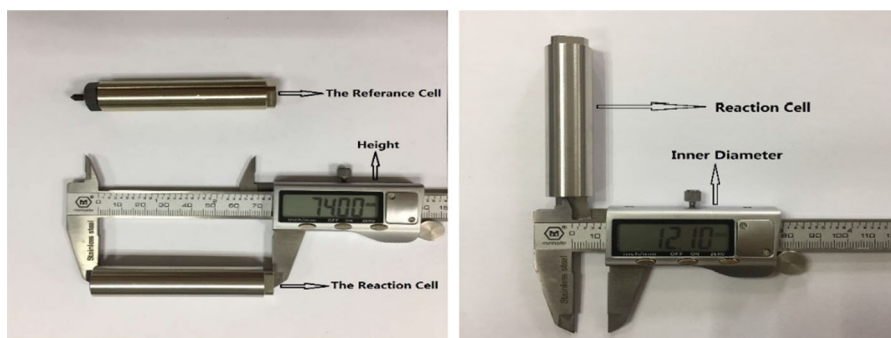


Fig. 3 The schematic of the reaction cell and the reference cell (Height = 74 mm; Inner diameter = 12.10 mm)

quantity of all the samples used in the tests was kept approximately 0.05 g by using an electron balance. Such a sample mass for NC in C80 calorimeter was selected by referring previous publications about energetic material degradation using C80 calorimeter [Sun et al. 2005, Ammonium nitrate 2 g; Katoh et al. 2010; Nitrocellulose 0.05 g; Guo et al. 2009, Multi-nitro Ester propellant 0.05 g].

Analysis

Chemical kinetic and thermodynamic parameters

The chemical kinetics of NC decomposition are usually described by the basic kinetic equation (Vyazovkin et al. 2011), as shown in Eq. (1).

$$\frac{d\alpha}{dt} = k(T)f(\alpha) \quad (1)$$

where α stands for the extent of reaction (α ranges from 0 to 1), $k(T)$ represents the rate constant, t is the time, and $f(\alpha)$ is the reaction mechanism function, which describes the relationship between the reaction rate and the degree of reaction. The value of α can be derived from the peak area of the C80 heat flow curves (Sun and Ding 2007), as described in Eq. (2).

$$\alpha = \frac{\int_{T_{onset}}^{T_r} \frac{dH}{dt} dt}{\int_{T_{onset}}^{T_{end}} \frac{dH}{dt} dt} \quad (T_{onset} < T_r \leq T_{end}) \quad (2)$$

where T_r represents the temperatures between the onset temperature and the end temperature. The reaction heat per mass is defined as ΔH , which can be obtained by integrating the heat release rate in a certain temperature range (Guo et al. 2009).

$$\Delta H = \frac{1}{M_0} \int_{T_{onset}}^{T_{end}} \frac{dH}{dt} dt \quad (3)$$

In most cases, the reaction rate constant of $k(T)$ is expressed by the Arrhenius equation, whose substitution into Eq. (1) yields.

$$\frac{d\alpha}{dt} = A \exp^{-\frac{E_a}{RT}} f(\alpha) \quad (4)$$

An advanced isoconversional method was proposed by Vyazovkin (Vyazovkin 2001) to evaluate the dependence of the activation energy on the extent of

conversion. According to the method, for a set of n experiments carried out at different heating rates, the activation energy (E_a) is determined at any particular value of α by finding the value of E_a which minimizes the function below.

$$\Phi(E_a) = \sum_{i=1}^n \sum_{j \neq i}^n \frac{J[E_a, T_i(t_{\alpha})]}{J[E_a, T_j(t_{\alpha})]} \quad (5)$$

where the subscripts i and j represent ordinal numbers of two experiments performed under different heating rates. Therefore α denotes the values related to a given extent of conversion. In this method, the integral is evaluated by Eq. (6).

$$J[E_a, T_i(t_{\alpha})] = \int_{t_{\alpha} - \Delta\alpha}^{t_{\alpha}} \exp\left[-\frac{E_a}{RT_i(t)}\right] dt \quad (6)$$

As shown in Eq. (6), the constancy of E_a is assumed for the small segment $\Delta\alpha$ and the integral J is evaluated from the experimental data using the trapezoid rule (Press et al. 1989). After obtaining the integral J values and substituting them in Eq. (5), the minimization is executed to determine E_a .

Evaluation of thermal hazard of nitrocellulose

The critical explosion temperature (T_b) is regarded as an important parameter to insure the safe storage or processing of energetic materials. It is defined as the lowest temperature under which the reaction will go through a transition from thermal decomposition to thermal explosion (Xu et al. 2008; Xue et al. 2010; Zhao et al. 2009). That is, there exists an index (T_b) to evaluate the thermal runaway condition. Based on the inflammation theory and the calculated kinetic parameters, the critical explosion temperature can be acquired by Eqs. (7) and (8) (Muravyev and Kiselev 2017; Trache and Khimeche 2013; Zhang et al. 1994).

$$T_e = T_{e0} + b\beta_i + c\beta_i^2 + d\beta_i^3, \quad i = 1 \sim 4 \quad (7)$$

$$T_b = \frac{E_A - \sqrt{E_A^2 - 4E_A R T_{e0}}}{2R} \quad (8)$$

where β_i is the heating rate, b , c , and d are the coefficients, R is the gas constant, the value (T_{e0}) of the onset temperature (T_e) corresponding to $\beta_i \rightarrow 0$ obtained by Eq. (7) and E_A is the activation energy which can be derived from reaction kinetic methods.

Results

Microstructures

Figure 4 shows SEM images of the four samples under different magnifications. At low magnifications (200 μm scale), the contrast among the four structures is even greater, especially in the degree of cotton fiber fracture. Moreover, at the medium magnifications (50 μm scale), the twining fibrous micro structures can be easily observed for the four samples while the surface roughness increases with the nitrogen content.

The space between the fibers in NC samples shows little difference. Further, at high magnifications (10 μm scale), it can be clearly seen that a smooth surface with only a few tiny cracks appeared in NC-11.43; NC-11.50 presents a slightly rough surface with small cracks; small cracks are further enlarged on the surface of NC-11.98; and NC-12.87 shows large cracks on a relatively rough surface. It is confirmed that the diameter of the fibers is approximately 20 μm . To the best of our knowledge, previous studies (Sovizi et al. 2009; He et al. 2017; Wei et al. 2017) have focused on the microstructures of the modified NC,

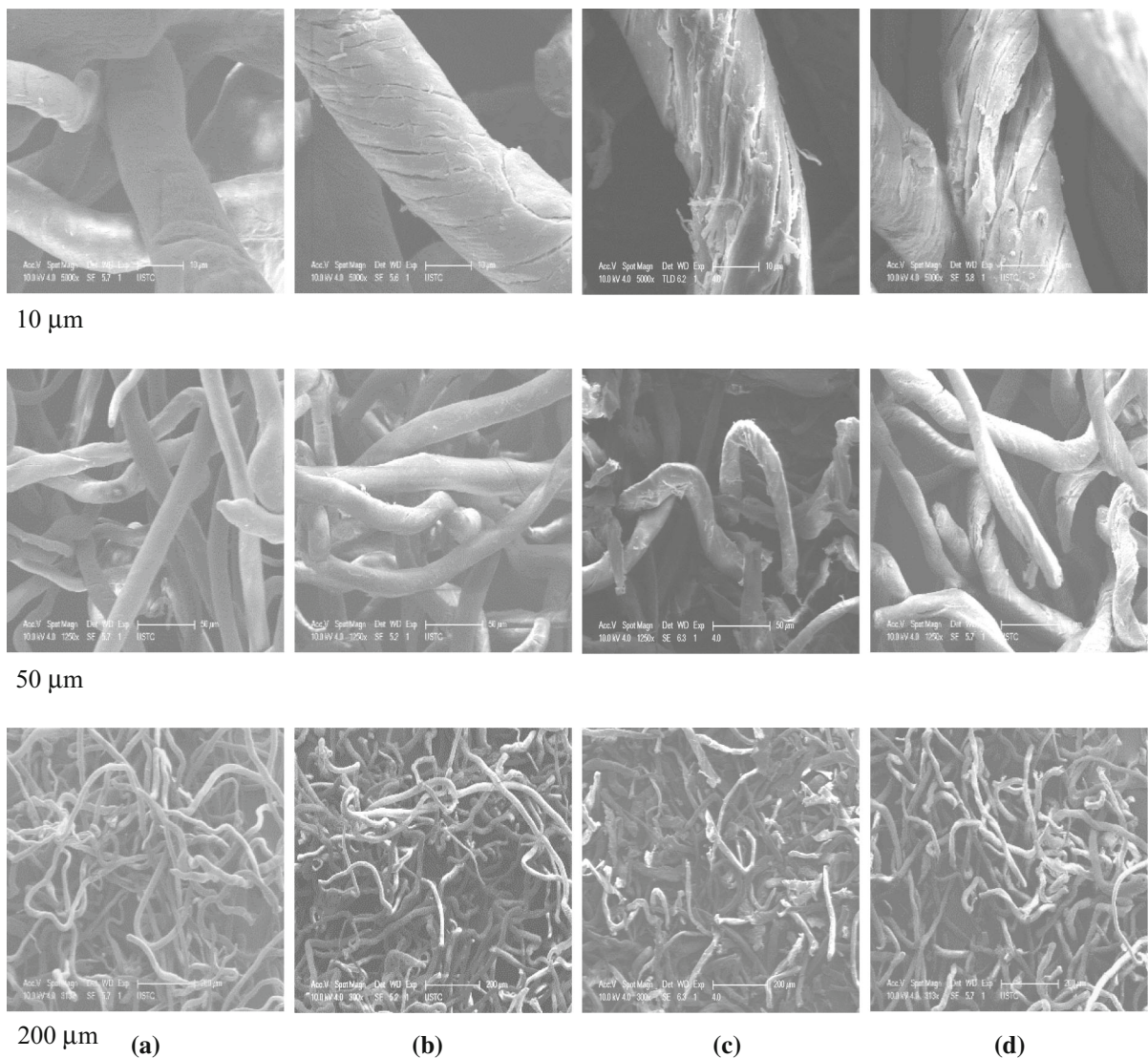


Fig. 4 SEM images of fibrous nitrocellulose with different nitrogen contents, **a** 11.43% (NC-11.43), **b** 11.50% (NC-11.50) **c** 11.98% (NC-11.98) and **d** 12.87% (NC-12.87)

believing that there are few differences in the structures of NC with different nitrogen contents. However, at the higher order of magnitude inspection, it was found that nitrogen content had a significant effect on the microstructures of NC. That is, the higher the nitrogen content is, the greater are the fractures. Zhang and Weeks confirmed that the burning rate of an NC sample increased with the increase of the specific surface area, allowing for more contact with atmospheric oxygen. And Hurley found that the cavity between the fibers could provide an effective diffusion space for the oxidizing gas to enter the interior of the sample. It is inferred that large surface cracks could increase the contact area between NC and oxygen, enlarge the specific contact area, thereby promoting the reaction (Hurley et al. 2015; Zhang and Weeks 2014).

Nonisothermal experiments by C80

Effect of nitrogen content on thermal characteristics of NC

Temperature rise experiments with constant heating rates of 0.2 °C/min, 0.4 °C/min, 0.6 °C/min and 0.8 °C/min were executed to research the effect of nitrogen content on the thermal characteristics of NC. Figure 5 shows the heat flow curves of NC samples with different nitrogen contents in an air atmosphere heated at 0.2 °C/min.

Only one exothermic peak was detected on each curve of Fig. 5. However, from the local enlarged picture, it was not hard to see that there existed an obvious turning point on heat flow curve of NC-12.87, where the heat release rate increased suddenly. The turning point is defined as the point on the heat flow curve with a characteristic temperature, which is the intersection temperature of the baseline and the tangent at the point where the heat flow curve rises abruptly. The point where the heat flow curve rises abruptly corresponds to the one at which the rate of change in heat release rate is the largest between the reaction start temperature and the peak temperature. And the baselines used are the experimental test ones (empty cell with no load) under different heating rates. According to the turning point, the whole process was divided into two stages. Before the turning point, the heat release rate increased slowly, but after that, the heat flow curve increased steeply to the peak point. To

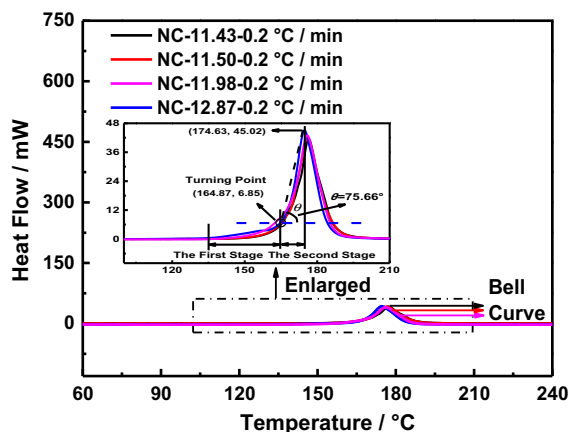


Fig. 5 Heat flow curves of NC with different nitrogen contents under the heating rate of 0.2 °C/min

describe the “steepness” of the second stage on the heat flow curve of NC-12.87, we defined a parameter θ that signified the angle between the straight line formed by the turning point to the peak point and the temperature axis. The value of θ was 75.66° on the heat curve of NC-12.87. In comparison, heat flow curves of NC-11.43, NC-11.50, and NC-11.98 presented bell-shaped characteristics, and the whole process seemed to be continuous without a turning point.

As for the thermal characteristics of NC under 0.4, 0.6, and 0.8 °C/min, the similar behaviors are shown in Figs. 6, 7 and 8. Taking the heat flow curves of NC-12.87 under 0.8 °C/min as an example (Fig. 8), it was found that the NC started to decompose at 164.76 °C, and then the heat flow increased slowly until 186.12 °C. After that, the heat flow went up at a linear rate ($\theta = 89.97^\circ$) to the maximum value of 659.30 mW at 186.48 °C. The heat flow curve after the turning point, which was enclosed with a line that was parallel to the temperature axis, formed the shape of a “right-angled triangle”. As the name implied, it stood for a kind of sharp peak which was more appropriate to describe the sudden increase of the heat release rate and could represent the thermal characteristic of the whole curve. Although the thermal behaviors of NC-11.43, NC-11.50, and NC-11.98 were similar and always appeared to be bell shaped, the specific decomposition parameters were quite different. It was found that with the increase of nitrogen content, the heat flow curves of the NC samples moved to lower temperatures, and the

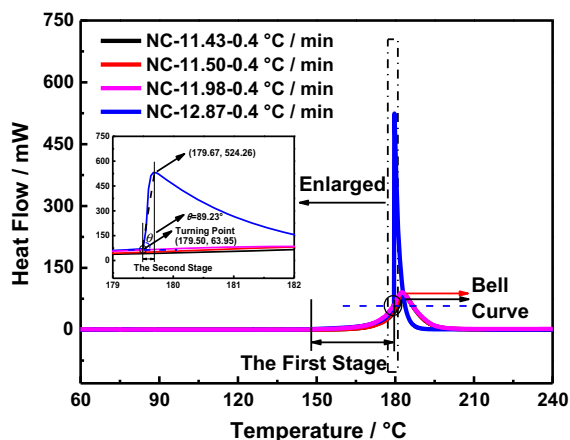


Fig. 6 Heat flow curves of NC with different nitrogen contents under the heating rate of 0.4 °C/min

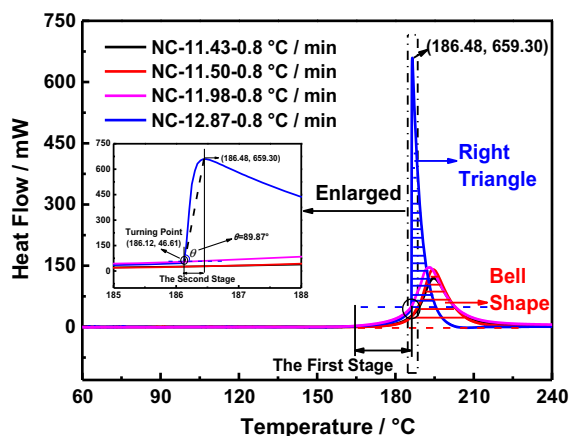


Fig. 8 Heat flow curves of NC with different nitrogen contents under the heating rate of 0.8 °C/min

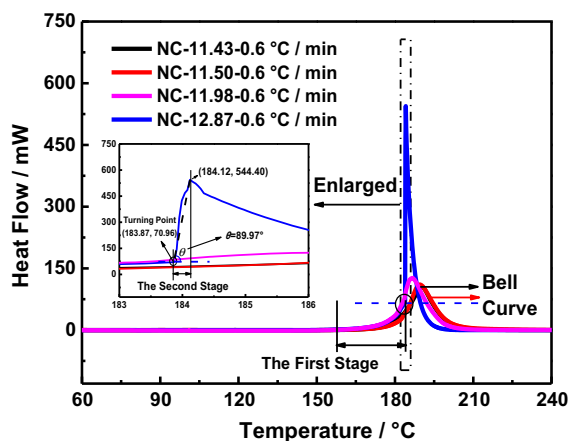


Fig. 7 Heat flow curves of NC with different nitrogen contents under the heating rate of 0.6 °C/min

maximum heat flows were increased. Moreover, it was clear that the shape of the heat flow curves changed from “bell shaped” to “right triangle”.

As an important parameter to describe the rate of change of the heat flow curves (Li et al. 2014; Wang et al. 2017), the change of the gradient of the heat release rate could be used to evaluate the thermal hazard. Figure 9 shows the derivative of the heat release rate of the NC samples under the heating rate of 0.8 °C/min. It was found that the parameter’s peak value of NC-12.87 was approximately 4000, which was 160 times larger than that of the NC-11.43, NC-11.50 and NC-11.98, whose peak values were only approximately 25. Additionally, the derivative of the heat release rate of NC-12.87 reached its maximum

value at a lower temperature than that of NC-11.43, NC-11.50 and NC-12.87. From the perspective of the heat flow curves change from “bell curves” to “right triangles”, and the rate of change of the heat release rate increases with the nitrogen content, it is inferred that the condition of 12.87% nitrogen content and 0.4 °C/min heating rate may be the critical state for 0.05 g sample, which can lead to combustion or explosion (Ning et al. 2004). To conclude, it implies that the higher the nitrogen content, the lower the peak temperature of the gradient of the heat release rate and the larger the corresponding peak value, thereby the greater the thermal hazard.

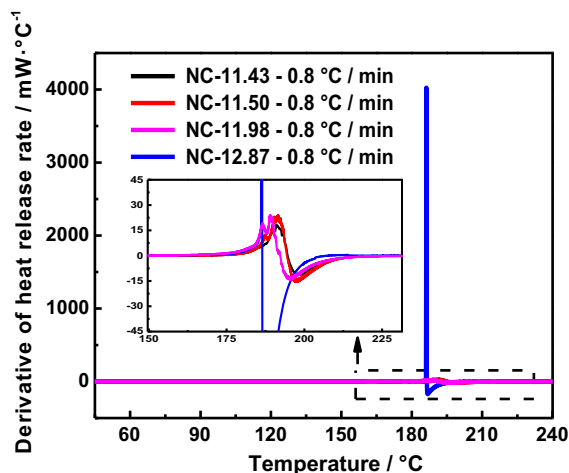


Fig. 9 Gradient of heat release rate of the NC samples under the heating rate of 0.8 °C/min

Effect of heating rate on thermal characteristic of NC

To investigate the effect of heating rate on the thermal characteristics of NC, Fig. 10 shows the onset temperature (T_{onset}), peak temperature (T_{peak}) and the maximum peak value (H_{peak}) of NC-11.43 under the heating rates of 0.2 °C/min, 0.4 °C/min, 0.6 °C/min, and 0.8 °C/min. Here the onset temperature is the point where the heat flow curve begins to deviate from the baseline (Jenkins and Donald 1998; Poel and Mathot 2006). And based on the Hess's Law (Mundhwa and Henni 2007), the whole decomposition reaction took a shorter time to complete under the higher heating rate, but the total heat release was almost the same, theoretically. Therefore, the maximum peak value (H_{peak}) increased by elevating the heating rate. Additionally, both the onset temperature (T_{onset}) and the peak temperature (T_{peak}) of NC increased with the heating rate in an air atmosphere. Based on the theoretical and experimental analysis above, and by comparison with the previous results (He et al. 2017), it was proven the maximum heat flow increased by elevating the heating rate, and the total heat release was almost unchanged.

From the experimental results of the lower heating rates ranging from 0.2 to 0.8 °C/min, it was found that the heat flow shape of “right triangles” of NC-12.87 was clearer with increasing heating rate. The variation values of the angle θ showed that the lowest heating rate in this experiment (0.2 °C/min) could make the reactant stay in the low temperature region for a long

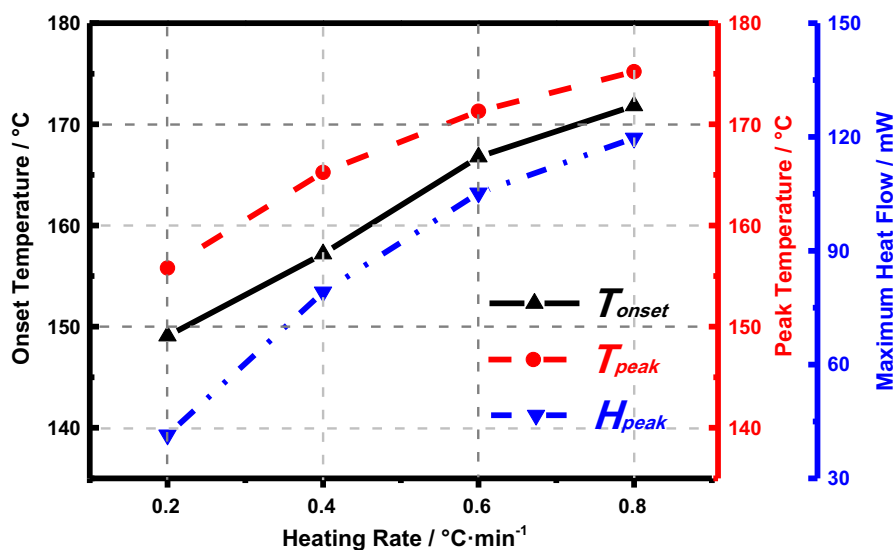
time, producing more intermediate product and promoting the reaction fully. The corresponding maximum heat flow was much lower, and the curve's shape was not clear, when compared with that of other three heating rates which showed the more obvious right-angled shape.

Isothermal experiments by C80

From the right-angled triangle characteristic of the heat flow curve of NC-12.87, a sharp increase of the heat release rate at a certain temperature was seen, which was closely related to the autocatalytic properties of NC. To examine whether the reaction was autocatalytic, isothermal experiments were carried out, which are widely considered as a reliable method to identify this process (Nguyen et al. 2017; Lv et al. 2013; Jankovic 2010).

Within the range of the onset temperatures, a higher temperature (approximately 175 °C) and a lower one (approximately 150 °C) were selected to conduct the isothermal experiments, as shown in Fig. 11. It was found that all the heat flow curves generally showed a “bell shape”, which met the criteria to verify the autocatalytic reaction and proved the reaction of NC was autocatalytic (Sun et al. 2017). And it is worth noting that the “peak envelope” in Fig. 11a seems to contain two or three small peaks, which might be the production of some intermediate products leading to the occurrence of several parallel reactions at the

Fig. 10 Onset temperature (T_{onset}), peak temperature (T_{peak}) and the maximum peak value (H_{peak}) of NC-11.43 under different heating rates



certain temperature (Ping et al. 2014; Jiang et al. 2015).

Moreover, compared with the other three samples under 175 °C (Fig. 11b), it is seen that the heat flow curve shape of NC-12.87 was more like the “right-angled triangle” rather than the common “bell shape”. This observation indicated that the autocatalytic trend of NC increased not only with the nitrogen content but also with the isothermal temperature. In addition, under the isothermal temperature approximately 150 °C (Fig. 11a), the time when the heat release rate of NC-11.43 reached to the maximum value was 19,175 s, which was three times longer than that of NC-12.87 (5725 s). Additionally, the heat release rate and the total heat release of the NC-12.87 was much higher than those of NC-11.43, NC-11.50, and NC-11.98. It is suggested that the NC with higher nitrogen content could reach its maximum heat release rate more quickly than those with lower nitrogen contents and thus bring a more substantial thermal hazard. From Fig. 11b, the time to the maximum heat release rate of the NC-12.87 was 1022 s, which was approximately 6 times shorter than that in Fig. 11a. This phenomenon showed that time to the maximum heat release rate could be decreased by elevating the isothermal temperature. To conclude, the autocatalytic property of NC became more obvious at higher isothermal temperatures. Additionally, the higher the nitrogen content is, the clearer is the autocatalytic characteristic, and the larger is the thermal hazard.

Discussion

Reaction kinetic and thermal dynamic parameters

According to experimental results, the reaction kinetics and thermodynamic parameters of NC with different nitrogen contents were obtained, as listed in Table 2. The results showed that with the increase of nitrogen content, the heat of reaction (ΔH) of the four samples increased, which indicated a larger nitrogen content could produce a larger heat release.

Figure 12 presents the activation energy of NC with different nitrogen contents at various conversion rates, using the advanced isothermal method by Vyazovkin (Vyazovkin 2001). The results show that when the conversion rate (α) is less than 10%, the activation energy (E_x) of NC decreases with increasing nitrogen content, which corresponds to the initial reaction stage before the turning point. After that, the values of E_x increase and show the opposite change from the beginning stage. As a kind of energetic material with autocatalytic characteristics, it starts slowly at the beginning of the reaction, and the reaction rate increases rapidly with the accumulation of the catalytic products. This study mainly focused on the thermal characteristics of NC in the initial reaction stage, the activation energy used for evaluating the critical explosion temperature was the average value (E_A) when the conversion rate was below 10%.

In conclusion, all these results revealed that the higher the nitrogen content, the larger the heat of

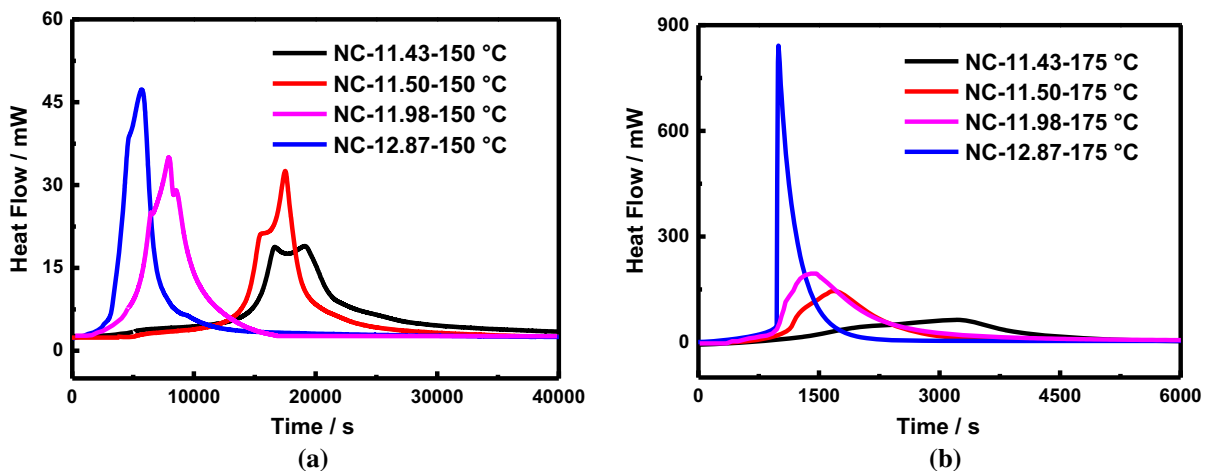
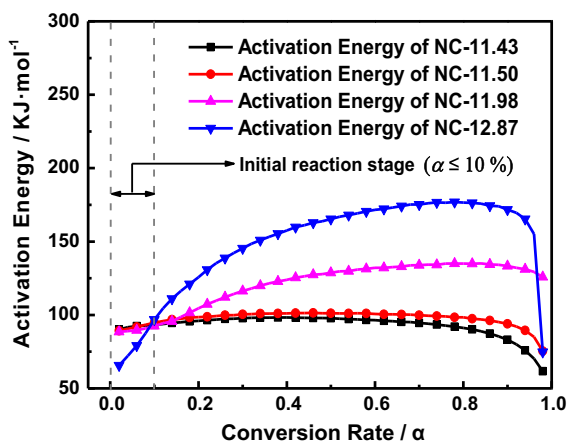


Fig. 11 Isothermal experiments of NC under 150 °C (a) and 175 °C (b) in air atmosphere

Table 2 Chemical kinetic parameters, thermal dynamic parameters and the critical explosion temperatures (T_b) of NC samples

Sample No.	ΔH (J g ⁻¹)	E_A (kJ mol ⁻¹)	T_{e0} (°C)	T_b (°C)
NC-11.43	2991.92 ± 195.28	91.40	137.92	154.56
NC-11.50	3038.79 ± 233.62	90.53	136.89	153.62
NC-11.98	3396.87 ± 149.19	89.03	126.62	142.77
NC-12.87	4073.46 ± 272.70	72.37	119.71	139.25

**Fig. 12** Activation energy of NC with different nitrogen contents at various conversion rates

reaction, and the easier and faster the reaction occurred.

Evaluation of thermal hazard

Based on the isothermal experimental results, the thermal decomposition process of NC was proven to be autocatalytic. Autocatalytic reactions mean that as long as the product was generated, it would act as the catalyst to promote the reaction to continue (Batten 1985; Tang et al. 2011; Trache and Tarchoun 2018). As the catalyst accumulated to a certain degree, the reaction rate could be accelerated sharply. Furthermore, the critical explosion temperatures (T_b) of the four samples NC samples were obtained, as shown in the last column of Table 2. It was found that the critical explosion temperature decreased with the increase of the nitrogen content. For example, the T_b for the NC with the nitrogen content 11.43 was approximately 154.56 °C, while the value of T_b was only 139.25 °C for NC-12.87. This is mainly because

the higher nitrogen content and its corresponding larger cracked microstructures could force the material into more contact with air and further prompt the reaction to proceed more easily (Hurley et al. 2015; Zhang and Weeks 2014). As a result, the NC with higher nitrogen content exhibits the more severe thermal hazard.

Conclusions

To investigate the effect of nitrogen content on the microstructure and thermal characteristics of nitrocellulose, a series of experimental tests were performed by SEM and C80. The relevant chemical kinetic and thermodynamic parameters of NC under low heating rates, including the heat of reaction (ΔH) and the activation energy (E_a), were obtained based on the Arrhenius equation and a theoretical model. Furthermore, the critical explosion temperatures (T_b) for NC with different nitrogen contents were also derived. The main conclusions are as follows:

1. SEM results of NC showed that the higher the nitrogen content is, the more cracks there are and the coarser is surface on the fibrous structures, which were favorable factors to enlarge the contact area between the substance and the air, thereby promoting the complete reaction.
2. Low heating rates helped to discover the “turning point” existing on the heat flow curves of NC with higher nitrogen contents. The maximum heat flow increased by elevating the heating rates.
3. Heat flow curves of NC changed from “bell shape” to “right triangles” might be attributed to the combustion or explosion process due to high nitrogen content accompanied with high heating rate. By elevating the nitrogen content, the maximum heat flow (H_{peak}), the derivative of the

heat release rate and the heat of reaction (ΔH) were increased. Additionally, the activation energy in the initial stage was reduced. All these results indicated that the larger the nitrogen content, the narrower the peak, the greater the heat release, and the easier the reaction.

4. By employing the isothermal method, the reaction of NC was verified to be autocatalytic. This autocatalytic characteristic increased with the nitrogen content and the isothermal temperature.
5. The critical explosion temperatures (T_b) of NC were decreased by increasing the nitrogen content. It was suggested that more care should be taken for NC with higher nitrogen contents during the processes of production, storage and transportation because of its more severe thermal hazard.

Acknowledgments This work is supported by the National Key Research and Development Plan (Projects Nos. 2016YFC0801502 and 2016YFC0801505). These supports are gratefully acknowledged.

References

- Abd-Elghany M, Klapötke TM, Elbeih A (2017) Thermal behavior and decomposition kinetics of Bis (2, 2, 2-trinitroethyl)-oxalate as a high energy dense oxidizer and its mixture with nitrocellulose. *Propellant Explos Pyrotech* 42:1373–1381. <https://doi.org/10.1002/prop.201700179>
- Batten JJ (1985) The agent of the autocatalytic thermal decomposition of aliphatic nitrate ester explosives. *Int J Chem Kinet* 17:1085–1090. <https://doi.org/10.1002/kin.550171005>
- Bessières D, Lafitte T, Daridon JL, Randzio SL (2005) High pressure thermal expansion of gases: measurements and calibration. *Thermochim Acta* 428:25–30. <https://doi.org/10.1016/j.tca.2004.09.020>
- Cuissinat C, Navard P, Heinze T (2008) Swelling and dissolution of cellulose, Part V: cellulose derivatives fibres in aqueous systems and ionic liquids. *Cellulose* 15:75–80. <https://doi.org/10.1007/s10570-007-9159-3>
- Guo S, Wang QS, Sun JH, Liao X, Wang ZS (2009) Study on the influence of moisture content on thermal stability of propellant. *J Hazard Mater* 168:536–541. <https://doi.org/10.1016/j.jhazmat.2009.02.073>
- He Y, He YP, Liu JH, Li P, Chen MY, Wei RC, Wang J (2017) Experimental study on the thermal decomposition and combustion characteristics of nitrocellulose with different alcohol humectants. *J Hazard Mater* 340:202–212. <https://doi.org/10.1016/j.jhazmat.2017.06.029>
- Hurley MJ, Gottuk DT, Hall JR Jr, Harada K, Kuligowski ED, Puchovsky M, Torero JL, Watts JM Jr, Wieczorek CJ (2015) *SFPE handbook of fire protection engineering*. Springer, Berlin
- Janković B (2010) The kinetic analysis of isothermal curing reaction of an unsaturated polyester resin: estimation of the density distribution function of the apparent activation energy. *Chem Eng J* 162:331–340. <https://doi.org/10.1016/j.cej.2010.05.010>
- Jenkins PJ, Donald AM (1998) Gelatinisation of starch: a combined SAXS/WAXS/DSC and SANS study. *Carbohydr Res* 308:133–147. [https://doi.org/10.1016/S0008-6215\(98\)00079-2](https://doi.org/10.1016/S0008-6215(98)00079-2)
- Jiang L, Xiao HH, He JJ, Sun Q, Gong L, Sun JH (2015) Application of genetic algorithm to pyrolysis of typical polymers. *Fuel Process Technol* 138:48–55. <https://doi.org/10.1016/j.fuproc.2015.05.001>
- Jiang L, He JJ, Sun JH (2018) Sample width and thickness effects on upward flame spread over PMMA surface. *J Hazard Mater* 342:114–120. <https://doi.org/10.1016/j.jhazmat.2017.08.022>
- Katoh K, Ito S, Kawaguchi S, Higashi E, Nakano K, Ogata Y, Wada Y (2010) Effect of heating rate on the thermal behavior of nitrocellulose. *J Therm Anal Calorim* 100:303–308. <https://doi.org/10.1007/s10973-009-0478-5>
- Krause H (2013) *Conversion concepts for commercial applications and disposal technologies of energetic systems*. Springer, Berlin
- Li KY, Huang X, Fleischmann C, Rein G, Ji J (2014) Pyrolysis of medium-density fiberboard: optimized search for kinetics scheme and parameters via a genetic algorithm driven by Kissinger's method. *Energy Fuels* 28:6130–6139. <https://doi.org/10.1021/ef501380c>
- Lin CP, Li JS, Tseng JM, Mannan MS (2016) Thermal runaway reaction for highly exothermic material in safe storage temperature. *J Loss Prev Proc* 40:259–265. <https://doi.org/10.1016/j.jlp.2016.01.006>
- Lv JY, Chen LP, Chen WH, Gao HS, Peng MJ (2013) Kinetic analysis and self-accelerating decomposition temperature (SADT) of dicumyl peroxide. *Process Saf Environ* 57:1:60–63. <https://doi.org/10.1016/j.tca.2013.08.029>
- Miyake A, Sumino M, Oka Y, Ogawa T, Iizuka Y (2000) Prediction and evaluation of the reactivity of self-reactive substances using microcalorimetries. *Thermochim Acta* 352:181–188. [https://doi.org/10.1016/S0040-6031\(99\)00465-7](https://doi.org/10.1016/S0040-6031(99)00465-7)
- Mundhwa M, Henni A (2007) Molar excess enthalpy for various alkanolamine(1) + water(2) systems at T = (298.15, 313.15, and 323.15) K. *J Chem Thermodyn* 39:1439–1451. <https://doi.org/10.1016/j.jct.2007.03.010>
- Muravyev NV, Kiselev VG (2017) Cheaper, faster, or better: are simple estimations of safety parameters of hazardous materials reliable? Comments on “thermal behaviors, nonisothermal decomposition reaction kinetics, thermal safety and burning rates of BTATz-CMDB propellant” by Zhao et al. (2010). *J Hazard Mater* 334:267–270. <https://doi.org/10.1016/j.jhazmat.2017.03.063>
- Nguyen GT, Tran KT, Pham TV, Nguyen HT (2017) Kinetic study of synthesis reaction of lignosulfonate using isothermal differential scanning calorimetry method. *Vietnam J Sci Technol* 55:493. <https://doi.org/10.15625/2525-2518/55/4/9029>
- Ning BK, Hu RZ, Zhang H, Xia ZM, Guo PJ, Liu R, Lu G, Jiang JY (2004) Estimation of the critical rate of temperature rise for thermal explosion of autocatalytic decomposing

- reaction of nitrocellulose using non-isothermal DSC. *Thermochim Acta* 416:47–50. <https://doi.org/10.1016/j.tca.2003.11.029>
- Onésippe C, Passe-Coutrin N, Toro F, Delvasto S, Bilba K, Arsène MA (2010) Sugar cane bagasse fibres reinforced cement composites: thermal considerations. *Compos Part A-Appl S* 41:549–556. <https://doi.org/10.1016/j.compositesa.2010.01.002>
- Ping P, Wang QS, Huang PF, Sun JH, Chen CH (2014) Thermal behaviour analysis of lithium-ion battery at elevated temperature using deconvolution method. *Appl Energy* 129:261–273. <https://doi.org/10.1016/j.apenergy.2014.04.092>
- Poel GV, Mathot VBF (2006) High-speed/high performance differential scanning calorimetry (HPer DSC): temperature calibration in the heating and cooling mode and minimization of thermal lag. *Thermochim Acta* 446:41–54. <https://doi.org/10.1016/j.tca.2006.02.022>
- Pourmortazavi SM, Hosseini SG, Rahimi-Nasrabadi M, Hajimirsadeghi SS, Momenian H (2009) Effect of nitrate content on thermal decomposition of nitrocellulose. *J Hazard Mater* 162:1141–1144. <https://doi.org/10.1016/j.jhazmat.2008.05.161>
- Press WH, Flannery BP, Teukolsky SA, Vetterling WT (1989) *Numerical recipes in pascal*. Cambridge University Press, Cambridge
- Shao ZQ, Wang WJ (2011) *Structure and properties of nitrocellulose*. National Defense Industry Press, Beijing (in Chinese)
- Sovizi MR, Hajimirsadeghi SS, Naderizadeh B (2009) Effect of particle size on thermal decomposition of nitrocellulose. *J Hazard Mater* 168:1134–1139. <https://doi.org/10.1016/j.jhazmat.2009.02.146>
- Sun JH, Ding H (2007) *Evaluation of the thermal risk of chemical substances*, 2nd edn. Science Press, Beijing (in Chinese)
- Sun JH, Sun ZH, Wang QS, Ding H, Wang T, Jiang CS (2005) Catalytic effects of inorganic acids on the decomposition of ammonium nitrate. *J Hazard Mater* 127:204–210. <https://doi.org/10.1016/j.jhazmat.2005.07.028>
- Sun ZD, Fu XL, Yu HJ, Fan XZ, Ju XH (2017) Theoretical study on stabilization mechanisms of nitrate esters using aromatic amines as stabilizers. *J Hazard Mater* 339:401–408. <https://doi.org/10.1016/j.jhazmat.2017.06.025>
- Tang Z, Ren Y, Yang L, Zhang TL, Qiao XJ, Zhang JG, Zhou ZN (2011) A new way to estimate the thermal decomposition mechanism function and thermal safety of RDX. *Chin J Explos Propellants* 34:19–25
- Trache D (2016) Comments on “thermal degradation behavior of hypochlorite-oxidized starch nanocrystals under different oxidized levels”. *Carbohydr Polym* 151:535–537. <https://doi.org/10.1016/j.carbpol.2016.05.106>
- Trache D, Khimeche K (2013) Study on the influence of ageing on thermal decomposition of double-base propellants and prediction of their in-use time. *Fire Mater* 37:328–336. <https://doi.org/10.1002/fam.2138>
- Trache D, Tarchoun AF (2018) Stabilizers for nitrate ester-based energetic materials and their mechanism of action: a state-of-the-art review. *J Mater Sci* 53:100–123. <https://doi.org/10.1007/s10853-017-1474-y>
- Trache D, Khimeche K, Mezroua A, Benziane M (2016) Physicochemical properties of microcrystalline nitrocellulose from Alfa grass fibres and its thermal stability. *J Therm Anal Calorim* 124:1485–1496. <https://doi.org/10.1007/s10973-016-5293-1>
- Trache D, Abdelaziz A, Siouani B (2017) A simple and linear isoconversional method to determine the pre-exponential factors and the mathematical reaction mechanism functions. *J Therm Anal Calorim* 128:335–348. <https://doi.org/10.1007/s10973-016-5962-0>
- Trache D, Maggi F, Palmucci I, DeLuca LT (2018) Thermal behavior and decomposition kinetics of composite solid propellants in the presence of amide burning rate suppressants. *J Therm Anal Calorim* 132:1601–1615. <https://doi.org/10.1007/s10973-018-7160-8>
- Vincent L, Barale S, Sandeau A, Castillo RV, Genet N, Sbirrazzuoli N (2017) Monitoring grease production by reaction calorimetry and thermoanalytical methods as an alternative to dropping point determination. *Energy Fuels* 31:11489–11494. <https://doi.org/10.1021/acs.energyfuels.7b01920>
- Vyazovkin S (2001) Modification of the integral isoconversional method to account for variation in the activation energy. *J Comput Chem* 22:178–183. [https://doi.org/10.1002/1096-987X\(20010130\)22:2%3c178::AID-JCC5%3e3.0.CO;2-%23](https://doi.org/10.1002/1096-987X(20010130)22:2%3c178::AID-JCC5%3e3.0.CO;2-%23)
- Vyazovkin S, Burnham AK, Criado JM, Pérez-Maqueda LA, Popescu C, Sbirrazzuoli N (2011) ICTAC kinetics committee recommendations for performing kinetic computations on thermal analysis data. *Thermochim Acta* 520:1–19. <https://doi.org/10.1016/j.tca.2011.03.034>
- Wang QS, Sun JH, Yao XL, Chen CH (2006) C80 calorimeter studies of the thermal behavior of LiPF₆ solutions. *J Solut Chem* 35:179–189. <https://doi.org/10.1007/s10953-006-9377-6>
- Wang QS, Ping P, Zhao XJ, Chu GQ, Sun JH, Chen CH (2012) Thermal runaway caused fire and explosion of lithium ion battery. *J Power Sources* 208:210–224. <https://doi.org/10.1016/j.jpowsour.2012.02.038>
- Wang XY, Fleischmann C, Spearpoint M, Li KY (2017) A simple hand calculation method to estimate the pyrolysis kinetics of plastic and wood materials. *Fire science and technology* 2015. Springer, Singapore, pp 455–462. https://doi.org/10.1007/978-981-10-0376-9_46
- Wei RC, He YP, Liu JH, He Y, Mi WZ, Yuen R, Wang J (2017) Experimental study on the fire properties of nitrocellulose with different structures. *Materials* 10:316. <https://doi.org/10.3390/ma10030316>
- Weir J (1946) Nitroglycerine and guncotton: a double centenary. *Nature* 158:83. <https://doi.org/10.1038/158083a0>
- Wu TQ, Chen HD, Wang QS, Sun JH (2018) Comparison analysis on the thermal runaway of lithium-ion battery under two heating modes. *J Hazard Mater*. <https://doi.org/10.1016/j.jhazmat.2017.11.022>
- Xinhua News Agency (2016) Tianjin Port “8.12” Ruihai dangerous goods warehouse special fire and explosion investigation report. <http://www.chinasafety.gov.cn/newpage/newfiles/201600812baogao.pdf>. (in Chinese)
- Xu KZ, Song JR, Zhao FQ, Ma HX, Gao HX, Chang CR, Ren YH, Hu RZ (2008) Thermal behavior, specific heat capacity and adiabatic time-to-explosion of G (FOX-7).

- J Hazard Mater 158:333–339. <https://doi.org/10.1016/j.jhazmat.2008.01.077>
- Xue L, Zhao FQ, Hu RZ, Gao HX (2010) A simple method to estimate the critical temperature of thermal explosion for energetic materials using nonisothermal DSC. J Energ Mater 28:17–34. <https://doi.org/10.1080/07370650903124518>
- Zhang X, Weeks BL (2014) Preparation of sub-micron nitro-cellulose particles for improved combustion behavior. J Hazard Mater 268:224–228. <https://doi.org/10.1016/j.jhazmat.2014.01.019>
- Zhang TL, Hu RZ, Xie Y, Li FP (1994) The estimation of critical temperatures of thermal explosion for energetic materials using non-isothermal DSC. Thermochim Acta 244:171–176. [https://doi.org/10.1016/0040-6031\(94\)80216-5](https://doi.org/10.1016/0040-6031(94)80216-5)
- Zhang YH, Shao ZQ, Gao KZ, Li J, Wu X, Wang WJ, Wang FJ, Liu YH (2014) Rheological characteristics of nitrate glycerol ether cellulose gel based on phase separation in ternary system. Cellulose 21:4135–4143. <https://doi.org/10.1007/s10570-014-0355-7>
- Zhao FQ, Hu RZ, Gao HX (2009) A simple method based on Harcourt-Esson's equation to estimate the critical temperature of thermal explosion for energetic materials using non-isothermal DSC. Chin J Chem 27:1067–1072. <https://doi.org/10.1002/cjoc.200990178>
- Zhou JH, Zheng YP, Liu JJ, Bing X, Hua JJ, Zhang HY (2016) A paper-based detection method of cancer cells using the photo-thermal effect of nanocomposite. J Pharm Biomed 117:333–337. <https://doi.org/10.1016/j.jpba.2015.09.017>